Sensors and Actuators A 312 (2020) 112106

Contents lists available at ScienceDirect

Sensors and Actuators A: Physical

journal homepage: www.elsevier.com/locate/sna

# Capacitive pressure sensor inlaid a porous dielectric layer of superelastic polydimethylsiloxane in conductive fabrics for detection of human motions

Siming Li, Ke Dong, Ruiqing Li, Xiayan Huang, Tianjiao Chen, Xueliang Xiao*

*Key laboratory of Eco-textiles, Ministry of Education, Jiangnan University, Wuxi, 214122, China*

ARTICLE INFO

*Article history:*
Received 18 March 2020
Received in revised form 21 May 2020
Accepted 23 May 2020
Available online 31 May 2020

*Keywords:*
Capacitive pressure sensor
Electromechanical performance
Porous dielectric layer
Super elasticity

ABSTRACT

Flexible, sensitive and largescale normal pressure sensors are in high demand of rapid development of healthcare and e-skin systems. In this paper, a new capacitive normal pressure sensor was fabricated based on a dielectric layer of superelastic polydimethylsiloxane (PDMS) with uniformly distributed micro-pores. The micro-pores were formed through vacuum-assisted infiltration of PDMS solution using sugar particles as porogen. Results showed that the PDMS layer with uniform micro-pores without sugar residue was successfully obtained. The developed sensor experimentally displayed a high elasticity, a large sensing pressure range (> 200 kPa), a high sensitivity (0.023 $kPa^{-1}$), a good hysteresis, a fast response (about 155 ms) and a good structural stability and durability for using more than 1000 cycles. Demonstrations of the fabricated sensor in detecting finger grabbing and plantar pressure were performed, indicating it a high potential in the future use of e-skin or rehabilitation monitoring system.

© 2020 Elsevier B.V. All rights reserved.

## 1. Introduction

Flexible pressure sensors have attracted much attention due to their excellent potential applications in wearable electronics and intelligent systems [1–3], which can be mounted on human skin or garments for continuously monitoring subtle or large human motions, such as electrocardiogram [4,5], pulse [6] and joint bending [7]. In recent years, rapid developments of medical diagnostic systems [8,9] and electronic skin systems [10,11] have driven higher demands for the good flexibility, sensitivity, lightweight and adaptability of pressure sensors. Flexible pressure sensors have also been explored based on different principles, including piezoresistive [12,13], capacitive [14–17] and piezoelectric [18] sensors. Among them, the capacitive pressure sensor is widely used because of its relatively simple structure, high sensitivity, low power consumption, good dynamic response performance and strong adaptability to harsh conditions such as high temperature, radiation and strong vibration [19].

For general capacitive pressure sensors by testing the variation of capacitance in response to any applied external pressure, the related equation governing the capacitance [20] is given by

$$C = \varepsilon_0 \varepsilon_r (A/d) \quad (1)$$

Where $\varepsilon_0$ is the space permittivity, $\varepsilon_r$ is the relative dielectric constant of the dielectric material, $A$ is the area of the capacitor and $d$ is the distance between two separated electrodes. The sensing performance of pressure sensors can be evaluated by a few characteristics, and in which the sensitivity has been considered as the most important one. For capacitive pressure sensors, capacitance varies with the deformation (thickness or area) of flexible dielectric layers such as polydimethylsiloxane (PDMS), ecoflex, dragon skin and thermoplastic elastomer (TPE) [21–24]. The sensitivity of such sensor usually depends on the flexibility of the dielectric layer. Among which, PDMS is one of the most commonly used elastomer due to its low Young's modulus, inherent transparency, environmental friendliness, excellent permeability, stability to environmental parameters like temperature and relative humidity, etc.

To date, many scholars have studied PDMS-based dielectric sensors. For example, Lei et al. [25,26] designed a capacitive tactile senor with PDMS as dielectric layer for plantar pressure detection. However, the unprocessed PDMS exhibits minor flexibility and sensitivity in the work. Therefore, various attempts were made by changing the inherent structure of PDMS in order to improve the sensitivity of pressure sensors. Tee et al. [27] utilized various thin

* Corresponding author.
*E-mail addresses:* xiao_xueliang@163.com, xiao_xueliang@jiangnan.edu.cn (X. Xiao).

https://doi.org/10.1016/j.sna.2020.112106
0924-4247/© 2020 Elsevier B.V. All rights reserved.

unstructured PDMS films as acting the dielectric layer and studied how types of geometries and spatial arrangement affect the mechanical sensitivity of the microstructures. Li et al. [28] obtained a wide range and high sensitivity of sensors by taking advantage of unique surface micro-pattern of lotus leaf as the template for electrodes and using polystyrene microspheres as the dielectric layer, while the photolithography processes were complicated and expensive. Another reported approach to improve the sensitivity is to form porous PDMS, which has been developed by various approaches, such as breath figures [17] and 3D printing [29]. However, compared with method by using porogen, these preparation methods are complicated in process and expensive in equipment, which is not conducive to wide application. Currently, many types of porogen have been used to fabricate porous PDMS, including salt [19], sugar [30], organic solvent [31] and polymer microbead stacking [32]. Considering raw materials, processing costs and ease of control of pore size and process, sugar/salt particle dissolution has become the most common manufacturing means for porous PDMS. For example, Sun et al. [21] reported a way to prepare porous polydimethylsiloxane/carbon nanofiber composites (p-PDMS/CNF) using carbon nanofiber coated sugar particles as a template. Li et al. [19] obtained a porous PDMS by vacuum-assisted infiltration process using different sizes of salt particles. The method of vacuum-assisted infiltration promoted to uniform distribution of pores and increased processing speed, the authors have also analyzed the PDMS structure. In addition, the sensitivity of as-made sensor was relatively low and practical application was absent. So far, the porous PDMS without sugar residue is still under exploration for its good elasticity, simple and fast manufacturing process.

In this study, in order to solve the practical application requirements of porous PDMS, an improved approach has been applied by optimizing vacuum-assisted infiltration parameters, in which different sizes of sugar particles were used as porogen for the low cost. Eventually, a high-performance porous PDMS film with uniform distribution of pores was successfully obtained in the same chemical structure of original PDMS. Afterwards, a capacitive pressure sensor was fabricated by using the porous PDMS as a dielectric layer, and the sensor was investigated for the sensing performance. Compared with previous studies [19,25,26], our developed sensor displayed multiple advantages such as a large range of sensing pressures (> 200 kPa), a relatively good sensitivity of 0.023 $kPa^{-1}$, excellent compression property, good hysteresis and a fast response time of 155 ms. The sensor remained stables for at least 1000 cycles under 10 and 80 kPa. Owing to the good performance, a finger sensor and a plantar sensor were fabricated and demonstrated for the sensing functions in practical.

## 2. Experimental contents

### 2.1. Fabrication of porous PDMS

Fig. 1 illustrates the fabrication process of a porous PDMS block using sugar particles as porogen. Here, before the fabrication process, sugar particles of a certain size distribution were precisely dry grinded and screened using a lapping machine and a suitable sieve. The sugar particles were then modified into a very narrow distribution of size and crystalline shape under a suitable temperature. The PDMS was prepared by mixing a base gel and a curing agent (American Dow Corning SYLGARD 184 Silicone Elastomer) in a weight ratio of 15:1. Then, the mixed solution was ultrasonic stirred for 5 min to achieve the aim of sufficient agitation. Due to the presence of air bubbles from stirring, the mixed liquid was placed in the vacuum drying oven to experience a degas process for 10–15 min. The prepared particles and PDMS solution were thoroughly mixed in the mold and a further degassing process was performed using a vacuum desiccator (60 °C for 2 h). In this step, the original air in the gap of sugar particles would be evacuated, and the liquid of PDMS would be vacuum-assisted compressed into these air voids. After fully filling, the porous PDMS could be obtained by demolding and immersing into deionized water (60 °C) for 6 h to dissolve the sugar particles away. Finally, a porous PDMS block was dried in an oven for 2 h to remove the moisture and cut into the size of 10 mm × 10 mm × 4.8 mm cuboids.

### 2.2. Fabrication of capacitive pressure sensor

The capacitive pressure sensor was fabricated using the porous superelastic PDMS film as a dielectric layer, a piece of conductive cloth tape (thickness: 0.1 mm, Shenzhen Huijia Co., Ltd., Shenzhen, China) was used as electrode. The conductive tape based on a plain woven fabric was electroplated with nickel on polyester yarns. Then, the tape was coated with a layer of copper on the nickel layer for higher conductivity via an electroplating device (Xinyouli Electromechanical Co. Ltd, Shenzhen, China). This process employed a common method, namely, acid copper electroplating for its low cost and easy to control. The required materials and process conditions were as follows: $CuSO_4$: 200 g/L, $H_2SO_4$: 70 ml/L, temperature: 25 °C, current density: 2.5 $A/dm^2$ and time: 3 min. Finally, a layer of nickel for anti-oxidation and anti-corrosion was electroplated on the copper layer. The coated thickness of nickel and copper layers were 15 nm and 30 nm, respectively. The combination of copper and nickel can provide with excellent electrical conductivity (0.02 $\Omega/m^2$). The conductive cloth tape in the size of 10 × 10 mm was attached to one side of PDMS dielectric layer. The fabrication process of capacitive pressure sensor is shown in Fig. 2. For more accurate measurement of electrical characteristics, copper wires were connected to the electrodes using the tape. The initial capacitive value of the pressure sensor was measured to be 2.8 pF.

### 2.3. Characterization and evaluation

The morphologies of sugar particles and micro pores of PDMS were both examined by a polarizing microscope (MoticBA310Pol, Beijing Hanmeng Zixing Instrument Co., Ltd., Beijing, China). The chemical information of the initial PDMS and modified porous PDMS were characterized by FTIR spectrometer (Nicolet-10, American Thermo Fisher Scientific Co., Ltd. (China), Shanghai, China) and X-ray diffractometer (D2 PHASER, Brooke AXS Co., Ltd., Berlin, Germany), respectively. The mechanical properties, such as compressions, were measured by a tensile tester (ALJ-50H, Fuzhou Aipu Instrument Co., Ltd., Fuzhou, China), which can give a measured relationship between thickness and external pressure.

A LCR meter (TH2829C, Tonghui Co., Ltd, Wuxi, China) was used to measure the capacitance of the fabricated sensor. The change of capacitance under an external pressure was measured using the LCR meter to investigate the effect of porous structure on the sensitivity and other characteristic parameters (hysteresis, stability, repeatability, etc.) of the sensor. The LCR meter is based on an electrical bridge structure. The LCR working principle is based on an equation of Q = C·U, where Q is the total amount of the stored electronic charges on the sensor surface, C is the capacitance of the sensor, and U is the current voltage between the two sensor surfaces. The LCR meter measures the transfer amount of charges during the sensor deformation under a certain external force, and U is set to be constant, thus, the C value and its variation of the sensor can be calculated according to the above equation. Then, C is an effective capacitance value of the sensor, which does not consider the detailed deformation of the sensor but the whole equivalent value of the integration of finite capacitance values. Here, the LCR meter can only give one channel of the capacitive

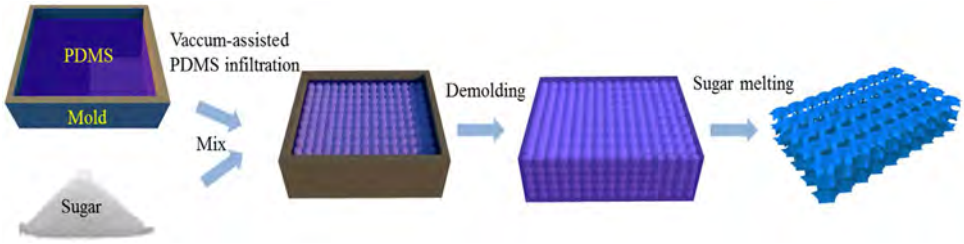


**Fig. 1.** Schematic of fabrication process of superelastic PDMS porous block.

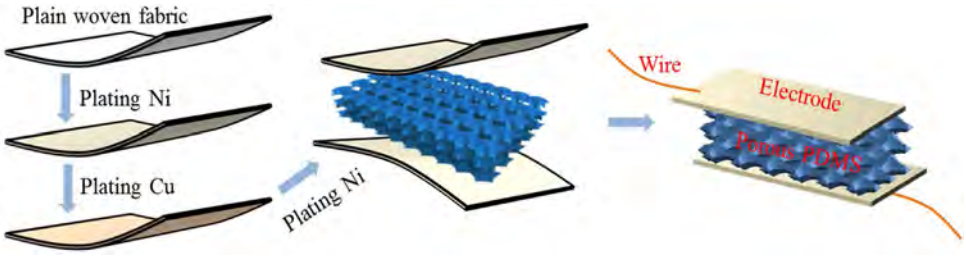


**Fig. 2.** Schematic illustration of the fabrication of capacitive pressure sensor.

signal for a single point. If more channels are required to obtain the variation of the capacitive signals for several compression points simultaneously, another open system is needed for the acquisition. Here, a hardware device (FDC1004QEVM, Yongdian Flagship Store, Wuxi, China) and corresponding self-software (Sensing Solutions EVM GUI) were used to record the capacitive signals of many compression points in real applications. In this work, we tried some demonstrated scenarios by tapping a table and grabbing a cup with sensors attached to fingers, and placing the sensor on the sole to detect plantar pressures.

The detailed information of LCR, hardware and software to record capacitive signals can be found in the supported document.

## 3. Results and discussions

### 3.1. Morphology of porous PDMS dielectric layer

The sugar particles were measured to have different sizes, which were divided into the ranges of 800–1000 μm, 600–800 μm and 400–600 μm (the samples were labeled as P-1, P-2 and P-3 accordingly) respectively, as shown in Fig. 3a–c. Here, the size is relatively larger than the previously reported work for sugar particles [19]. The larger size of sugar particles is believed to benefit the increase of the PDMS porosity. In the natural state, the sugar particles are randomly arranged although the neighboring sugar particles might contact each other under the natural stacking effect. However, this status is easier unbalanced during the filling of PDMS liquid considering the relatively smaller contact area and weaker contact force using larger sugar particles [19]. In order to improve the interconnectivity of PDMS and dissolution rate of sugar particles, a sufficient amount of sugar (the same volume as PDMS) with larger particle size was used.

Fig. 3d–f shows the microscope images of generated porous PDMS, the red elliptical marks indicate the formed pore sizes. It is obvious that the porous PDMS block from the larger size of sugar particles has a larger pore size. However, the pore sizes of PDMS are 700–900 μm, 500–700 μm and 300–500 μm respectively, which are smaller than the sizes of corresponding particles. This may be attributed to the potential shrinkage of PDMS after cooling from 60 °C in making PDMS and sugar solutions. In addition to the simple planar, the porous PDMS block can achieve relatively three-dimensional complex structures, demonstrating a strong structuring capability. This unique feature will undoubtedly benefit some practical applications. The real images of porous PDMS are displayed in Fig. 3g–i, in which the P-1 with largest pores is more transparent than others in comparison with the appearance due to the more uniform size of micro-pores obtained in P-1.

### 3.2. Chemical structure of PDMS samples

The inherent information of pure PDMS (which was labeled as P) and porous PDMS (P-1, P-2, P-3) with different pore sizes were characterized by FTIR and XRD. Here, FTIR was employed in characterizing the chemical interaction of molecules in pure and porous PDMS, respectively, as shown in Fig. 4a. Except for a falling curve in P-1, P-2 and P-3 between 3500 $cm^{-1}$ and 3000 $cm^{-1}$, which means the residual moisture in PDMS, the four curves display nearly the same characteristic peaks.

The XRD patterns of PDMS samples are shown in Fig. 4b. The principal strong diffraction peak of pure PDMS and P-1 samples at the abscissa of $2\theta = 21.98^{\circ}$ suggest their high degree of crystallinity (P-2 and P-3 show the same curves). Thus, it can be seen from the comparison that sugar particles are completely dissolved, and the presence of porous structure does not affect the chemical structures and crystalline phases of PDMS.

### 3.3. Working principle of capacitive pressure sensor

The sensitivity ($S$) of a capacitive pressure sensor is generally defined as Eq. (2):

$$S = \frac{\Delta C/C_0}{\Delta P} \tag{2}$$

Where $\Delta P$ represents the change of the applied pressure, $\Delta C$ and $C_0$ denote the relative change of the capacitance and the original capacitance, respectively. Thus, the sample thickness is the key factor to the capacitance change ratio ($\Delta C/C_0$) that would be affected easily by external pressure. Here, a detailed analysis of the compression property is investigated for the porous PDMS samples with different pore sizes. Fig. 5a illustrates the structure from the side and top views and the photograph of the pressure sensor. Fig. 5b displays the relationship of thickness and applied pressure. In practice, when an increased pressure is applied to the PDMS in the normal direction, its thickness is decreased rapidly at the beginning

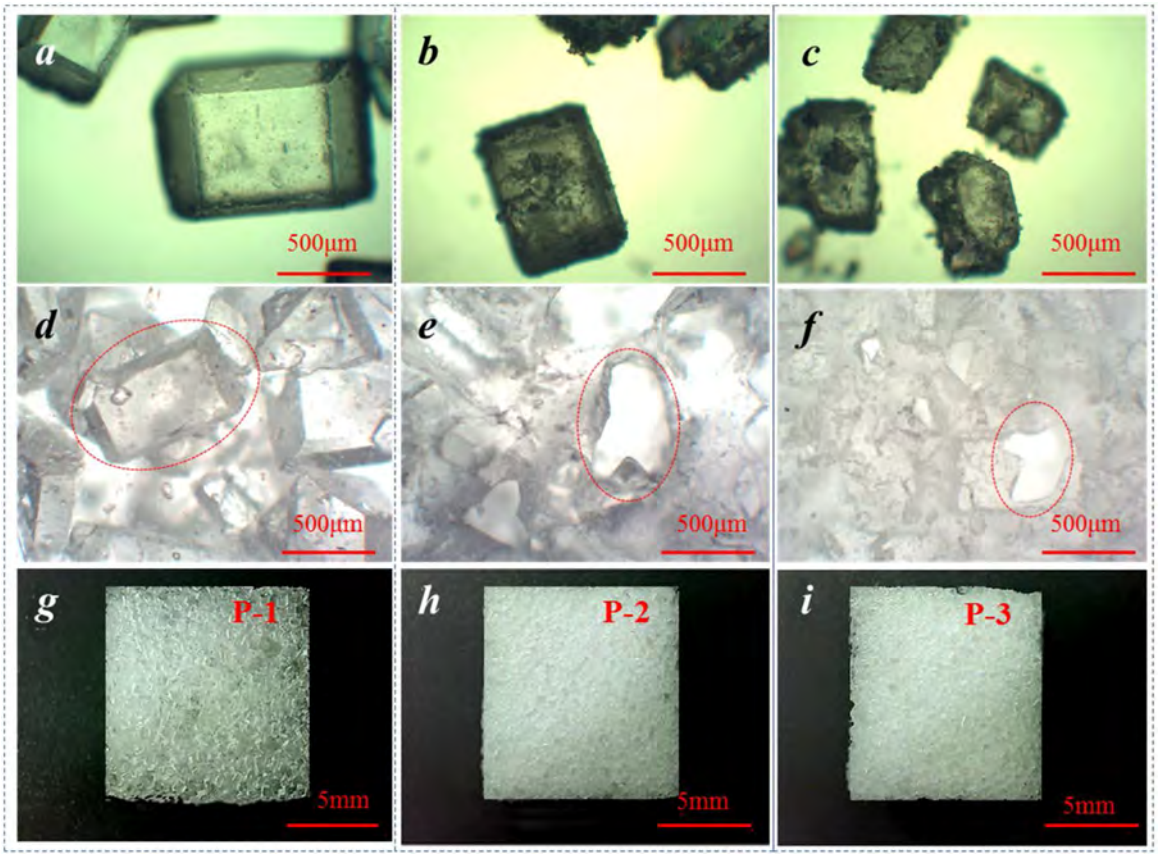


**Fig. 3.** Morphologies of, a–c) Microscope images of sugar particles with different sugar sizes, d–f) Microscope images of porous PDMS (P-1, P-2, P-3) with different pore sizes, g–i) real images of porous PDMS (P-1, P-2, P-3) with different transparencies.

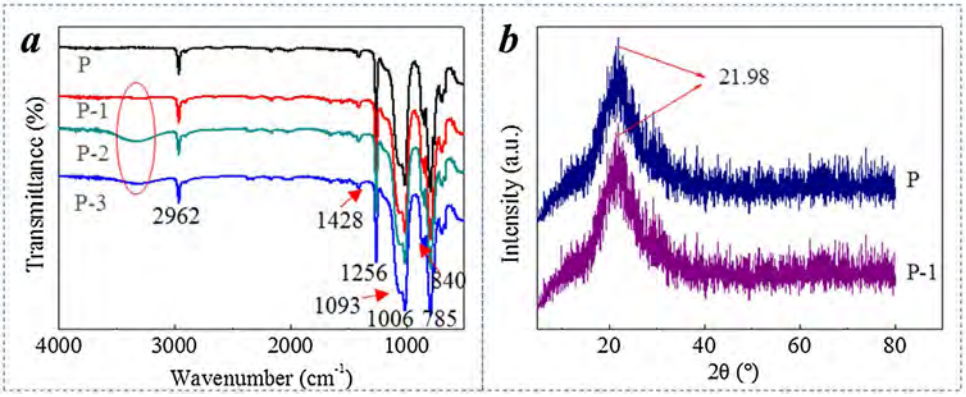


**Fig. 4.** Characterizations of PDMS samples, a) FTIR spectra of PDMS (P, P-1, P-2, P-3), b) XRD patterns of PDMS (P, P-1).

and afterwards slowly. Two empirical equations for the variation of thickness ($T$) under an increased pressure ($\Delta P$) are given as Eqs. (3) and (4) [13,33]:

$$T = T_0 \times e^{-f(\beta)} \tag{3}$$

$$\Delta P = \frac{\in}{(T_0 - T)^3} \tag{4}$$

Where $T_0$ is the original thickness, $T$ is the thickness under a pressure of $P$, $\beta$ and $\in$ are the fitting factors depending on the materials and structures used in the pressure sensor. To illustrate the relationship between thickness and pressure, we measured the real relationship of PDMS samples, and four curves are obtained as shown in Fig. 5c in similarity to Fig. 5b. Besides, Fig. 5c indicates that the porous PDMS is more easily deformed under compression with the increase of pore size due to the increased porosity. Fig. 5d shows a single compression behavior for the test. In general, the tensile tester (compression mode) gives the measured load (compression force, N) on the sensor sample, a transfer process is carried out for obtaining the pressure by using the reading load divided by the sensor surface size (area, $m^2$). Here, it is assumed that the sensor surface size is constant during the compression test. Therefore, the force direction of compression must be perpendicular to the sensor surface, and the force of compression is assumed to distribute evenly on the sensor surface.

Fig. 5c shows that the measured thickness of the sensor decreases in regularity under an increase of applied pressure, which would affect the change of sensitivity. The main reason is the shape change of micro pores inside PDMS under pressure. The whole

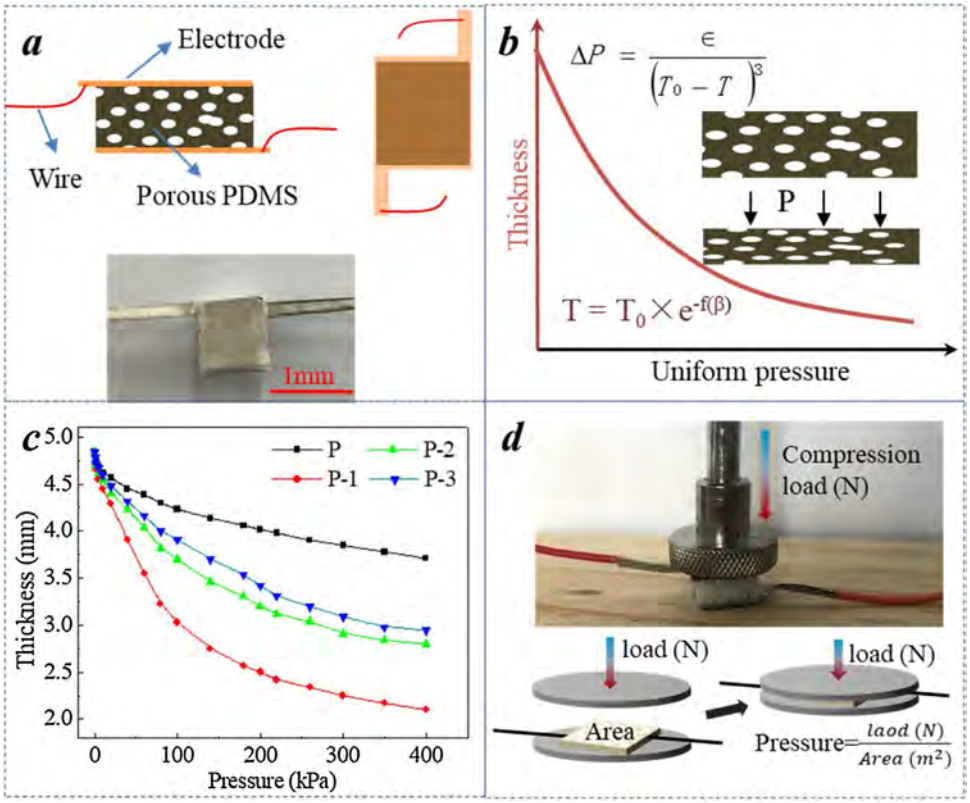


**Fig. 5.** The capacitive pressure sensor, a) The structure (including side view and top view) and the photograph of the sensor, b) decline relationship of PDMS thickness ($T_0$ to $T$) with applied pressure $\Delta P$, the inset shows empirical equations, c) the experimentally measured relationship of the thickness and applied pressure for four PDMS, d) real image of the sensor in a single compression behavior and the corresponding illustration of pressure acquisition.

Young's modulus ($E$) of the porous PDMS can be explained by Eq. (5) [31]:

$$E_{\text{total}} = aE_{\text{pores}} + bE_{PDMS} \tag{5}$$

Where a and b are the constants, and 0 < a, b < 1. The original $E$ of porous PDMS is much smaller than the solid PDMS as the $E$ of pores can be negligible. Therefore, when pressure is initially applied, the thickness drops rapidly until the pores disappear. Then, the thickness still decreases because the porous PDMS has the same $E$ value as solid PDMS. The increased pore size makes this phenomenon more pronounced, and the capacitance change ratio ($\Delta C/C_0$) of the pressure sensor would be more evident.

### 3.4. Electromechanical performance

Sensitivity ($S$) is an important characteristic parameter of a capacitive sensor. Fig. 6a shows four measured curves of the capacitance change ratio ($\Delta C/C_0$) along with the increased external pressures for different pore sizes of PDMS samples. The sensitivity of a capacitive pressure sensor is defined as the slope of the curve. As can be seen from the graph, $S$ is characterized by two consecutive regions with different values, which is compatible with the compression performance. That is, the ratio in the low pressure range (P < 20 kPa) is sensitive to the pressure, as shown in Fig. 6b. While $S$ changes slowly as the pressure increases (P > 20 kPa) and it is getting to zero in the high pressure range (P > 200 kPa). Therefore, the sensitivity of the pressure sensor is increased as the pore size and porosity are increased, because a larger size of pore raises the elastic range, and makes the porous PDMS sample to be more easily compressed. In the low-pressure region, the sensitivities were measured to be 0.006, 0.015, 0.017 and 0.023 $kPa^{-1}$ for P, P-3, P-2 and P-1, respectively, as shown in Fig. 6c. Therefore, it is included that a larger pore size can improve the deformability of PDMS, resulting in a higher sensitivity. Here, even though the sensitivity (especially in high-pressure region) is still small, it tends to increase with an increased pore size. Fig. 6d presents the $\Delta C/C_0$ curves of the pressure sensor based on P, P-1, P-2 and P-3 as dielectric layers under 20 kPa, showing that the pressure sensor has stable continuous responses for external pressure with different porosity of PDMSs.

Table 1 compares the key parameters (including $S$ and pressure range) among several capacitive pressure sensors using different PDMSs as their dielectric layers. The prepared pressure sensor using porous PDMS in this work displays a wider sensing range for pressures with higher $S$ values, indicating the superiority of the developed porous PDMS as a dielectric layer for pressure sensor. In comparison with Ref.19 that utilizing the same method, the sensor of this study shows a relatively larger monitoring range of normal pressures and a higher sensitivity.

In order to further study the sensing performance of the as-made capacitive pressure sensor, P-1 as dielectric layer is utilized as a sensor example to study its hysteresis, stability, repeatability and response time, respectively. Hysteresis refers to the consistency of forward and reverse strokes of a sensor. Normally, the sensor needs to work under dynamic pressure, and there would be an error if the sensor produces an unrecoverable deformation. Fig. 7a exhibits the measured hysteresis curves for the pressure sensor from a consecutive loading- unloading cycle. A negligible hysteresis is observed, indicating that the sensor has reliability and accuracy in obtaining pressure signals. The sensor is also operated stably, ensuring reliability even under continuous pressure loading/unloading cycles as shown in Fig. 7b. It can be observed that the corresponding capacitance ratios of pressure sensor under dif-

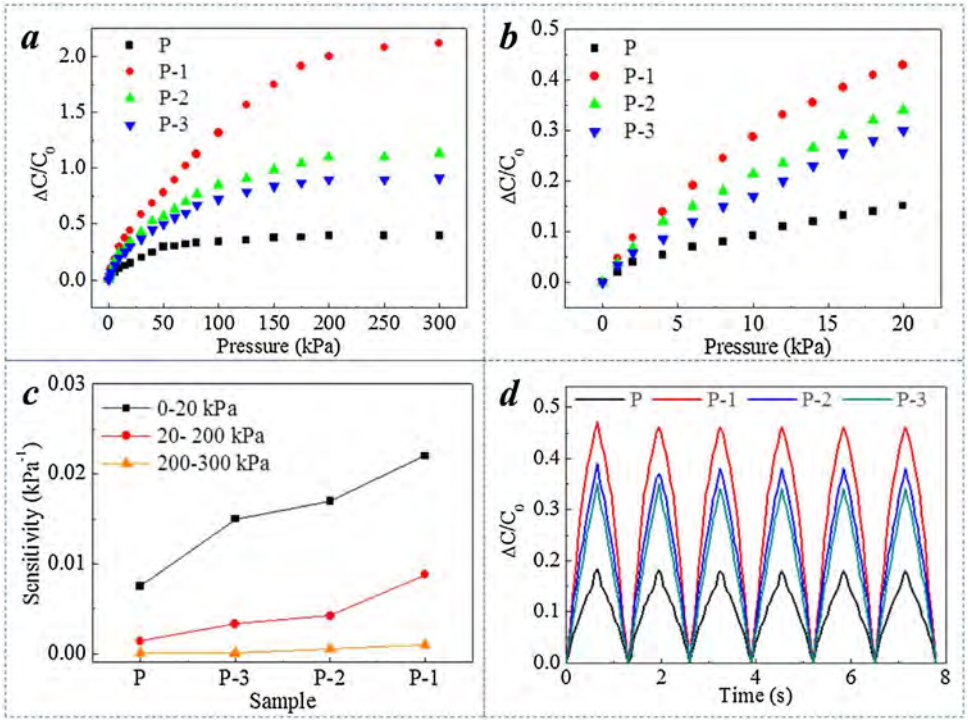


**Fig. 6.** Relative capacitance change ratio ($\Delta C/C_0$) versus pressure, a) 0–300 kPa and b) 0–20 kPa of four sensors based on P, P-1, P-2 and P-3, c) sensitivities as a function of sensors at the pressures of 0–20 kPa, 20–200 kPa and 200–300 kPa, d) $\Delta C/C_0$ curves of pressure sensor based on P, P-1, P-2 and P-3 as dielectric layer under 20 kPa.

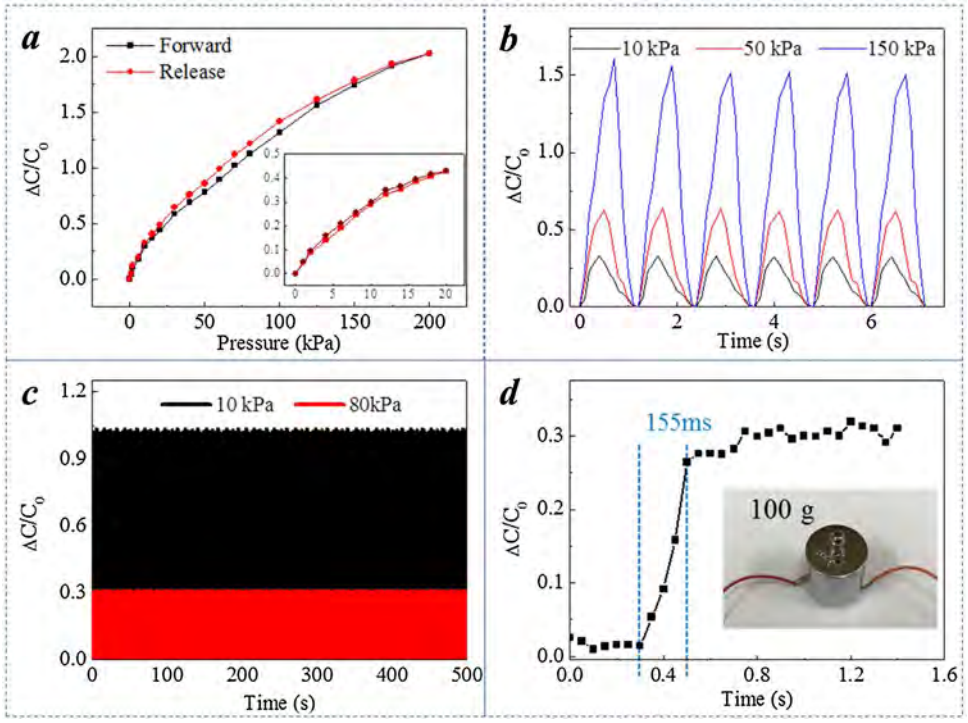


**Fig. 7.** a) $\Delta C/C_0$ curves of the pressure sensor from consecutive linear loading-unloading cycles of pressure, b) $\Delta C/C_0$ curves of the pressure sensor under different pressure (10, 50, 150 kPa), c) durability test under a pressure of 5 and 20 kPa, d) instant response of pressure sensor (under a weight 100 g), which shows response times of 155 ms.

ferent pressures of 10, 50, 150 kPa are 0.25, 0.6 and 1.5, respectively. The stability and repeatability of the sensor are measured through repeated loading-unloading for 1000 cycles, as shown in Fig. 7c. The relative capacitance change ratio of the pressure sensor is stably maintained without any remarkable degradation when applied pressures of 10 kPa and 80 kPa are loaded and unloaded repeatedly. Furthermore, Fig. 7d shows that the pressure sensor can detect a normal pressure with a fast response time of 155 ms when a weight of 100 g is placed on the sensor. Therefore, it is concluded that the sensor is fast responsive, highly durable and stable against any repeated mechanical pressure, which indicates a great potential use in detection of large-amplitude human motions.

**Table 1**
Comparison of the sensitivity and sensing pressure range for a few capacitive pressure sensors using PDMS as their dielectric layers.

| Electrode | Dielectric | Pressure ranges (kPa) | Sensitivities ($kPa^{-1}$) | Ref. |
|---|---|---|---|---|
| Electrode plates | Porous PDMS | 12 | 0.0107 | [19] |
| FPCB | Solid PDMS | 1000 | 0.00224 | [25] |
| Cu | Solid PDMS | 945 | 0.0016 | [26] |
| Al fabric | Porous PDMS | 0.2 | 0.813 | [32] |
| Copper plates | Microstructured PDMS | 6 | 0.1851 | [34] |
| Conductive cloth tape | Porous PDMS | 200 | 0.023 | This work |

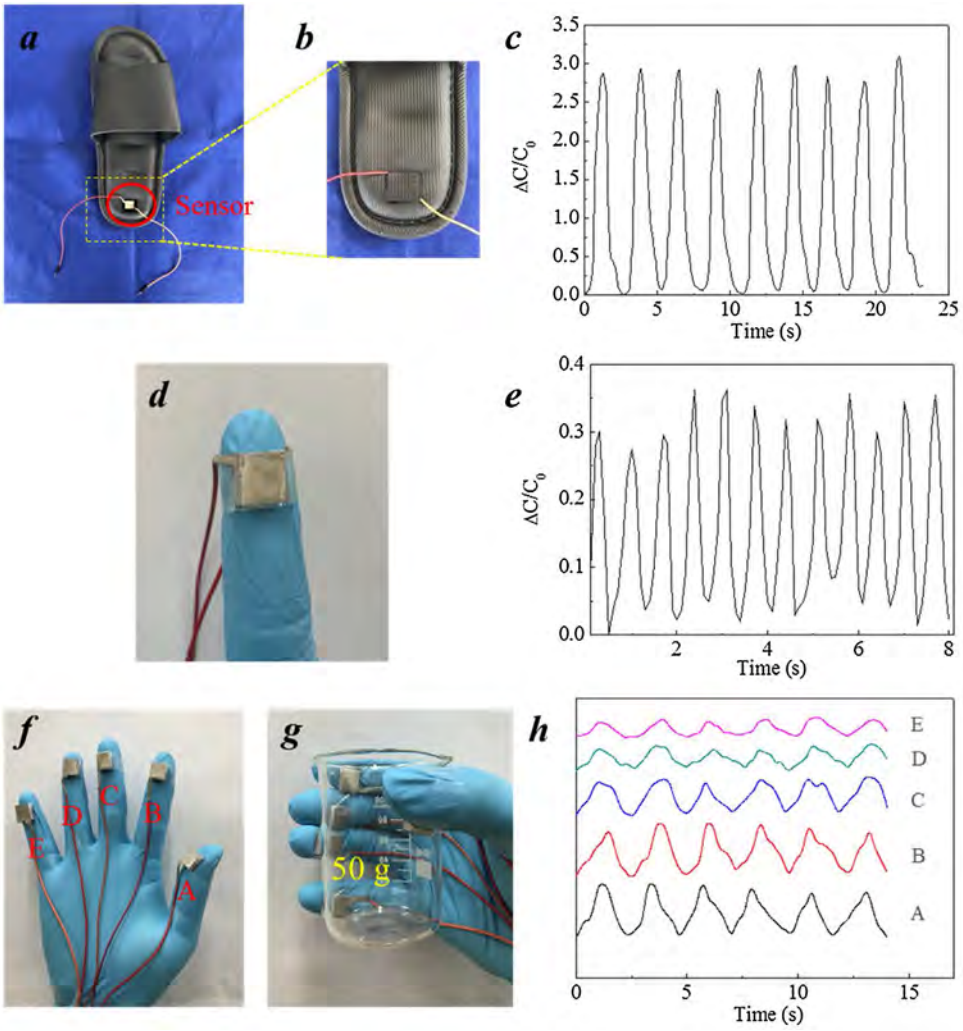


**Fig. 8.** Demonstrations of a, b) sensor applied to the sole of a shoe to record the sensor's response and c) $\Delta C/C_0$ curves during walking (tester: 70 kg), d) a photograph of a sensor attached to a finger and e) $\Delta C/C_0$ curves in gentle tapping, f, g) five sensors on each finger for grabbing a beaker and h) $\Delta C/C_0$ curves trend of different fingers in grabbing.

## 4. Application of the sensor in human motion detection

Upon characterization of various parameters of the sensor, a further test of the relationship of dynamic loading and capacitance change ratio is performed to analyze the ability of efficiently response to a time-varied mechanical loading. To achieve this, a hole was dug in a PVC slipper (15 × 15 × 10 mm) and the self-developed sensor was mounted on the heel position of the slipper to record the capacitance change over time during walking for plantar pressure detection as shown in Fig. 8a–b. Then, the test can record the walking process of a tester within 25 s (volunteer weight: 70 kg, walking frequency: 0.4 Hz), and the tester keep the foot off or on the ground during walking. The testing result is shown in Fig. 8c, in which the weight recorded to the sensor varies from 0 kPa to about 350 kPa that is in similarity with the investigation of previous work [34], indicating that the sensor as a part of a gait analysis device can effectively detect some dynamic pressure changes.

The measurement of static and dynamic pressure from finger was also demonstrated in the form of a skin attachment sensor. Firstly, a sensor was attached onto a finger and consecutively tapped a table surface with the finger (tapping frequency: 1.5 Hz) as shown in Fig. 8d and the result is displayed in Fig. 8e, illustrating that the sensor can detect the finger tapping well. Furthermore, five more sensors were attached to a tester's right hand fingers to pick up a 50 g beaker as shown in Fig. 8f and g. The tester repeatedly picked up and dropped the beaker, and the $\Delta C/C_0$ ratio was measured simultaneously from each finger (Fig. 8h). According to

the measured $\Delta C/C_0$ curves and their trends from different fingers in grabbing, the ratio appeared the highest at the finger A and B and lowest at the finger E. The peak value of $\Delta C/C_0$ produced by each finger was A (0.8), B (0.8), C (0.6), D (0.3) and E (0.2), respectively. This means the tester gives the thumb and index finger the highest and the smallest forces while grabbing the beaker, which is consistent with commonsense.

From the demonstrations, it is noted that the demonstrated scenarios are all in the similar sensing conditions, that are, the compression force acting area (tripe of finger or heel) is larger than the sensor surface area, as is also shown in Fig. 5d of the testing situation, this kind of application scenarios ensure a relatively uniform deformation of the sensor surface that means the difference of deformations at the central and edge of sensor surfaces can be ignored due to the compression cover of acting area. The pressure is then obtained from the exerted force divided by the sensor surface area which is assumed as constant. However, obviously, the smaller size of the sensor would have smaller measure errors for the reason of more ignored uneven deformations and the edge effect of electrical field for accurate capacitance. From the demonstrations of pressure detection of plantar and fingers, it is concluded that the proposed pressure sensor exhibits excellent stability and repeatability, which shows a high potential to use in artificial skin and rehabilitation monitoring. Next stage, the sensor will be explored for the relationship of measured pressure, real pressure and the specific structure and material parameters of the sensor.

## 5. Conclusions

In summary, a flexible capacitive pressure sensor was fabricated using a porous PDMS block as the dielectric layer with uniformly distributed micro-pores. The porous PDMS was obtained by utilizing processed sugar particles as porogen and vacuum assisted to promote the fabrication process. The production process, morphology, chemical and physical properties examined by FTIR and XRD, and the compression of the porous PDMS were characterized in detail. Experimental results showed that the porous PDMS exhibited high elasticity, no sugar residue and good interconnectivity. Subsequently, a capacitive sensor was assembled by attaching a conductive cloth tape to the sides of the PDMS dielectric layer.

The capacitive pressure sensors displayed various great properties including high elasticity, a large test range of pressures more than 200 kPa, a relatively good sensitivity of 0.023 $kPa^{-1}$, good hysteresis, a response time about 155 ms under a pressure of 100 g weight. In addition, the sensor remained stable for at least 1000 cycles of compression behaviors under 10 and 80 kPa, respectively. In practical applications, the plantar and finger sensors were demonstrated by walking and tapping a table slightly and grabbing a 50 g beaker, respectively. The simple process and low-cost flexible capacitive pressure sensor based on the self-developed porous PDMS as the dielectric layer implies a great potentiality use in e-skin sensing system and future rehabilitation monitoring.

## Author statement

S. Li, K. Dong and R. Li conceived the idea and designed the experiment. S. Li, T. Chen and X. Huang fabricated the pressure sensor. S. Li and X. Xiao analyzed the experimental results and wrote the paper.

## Declaration of Competing Interest

The authors declare no conflict of interest.

## Acknowledgement

This work was supported by the National Natural Science Foundation of China (Grant No. 51703083).

## Appendix A. Supplementary data

Supplementary material related to this article can be found, in the online version, at doi:https://doi.org/10.1016/j.sna.2020.112106.

## References

[1] M. Amjadi, K.-U. Kyung, I. Park, M. Sitti, Stretchable, skin-mountable, and wearable strain sensors and their potential applications: a review, Adv. Funct. Mater. 26 (2016) 1678–1698.
[2] C. Wang, K. Xia, H. Wang, X. Liang, Z. Yin, Y. Zhang, Advanced carbon for flexible and wearable electronics, Adv. Mater. 31 (2019), 1801072.
[3] T. Tran Quang, N.-E. Lee, Flexible and stretchable physical sensor integrated platforms for wearable human-activity monitoring and personal healthcare, Adv. Mater. 28 (2016) 4338–4372.
[4] X. Xiao, G. Wu, H. Zhou, K. Qian, J. Hu, Preparation and property evaluation of conductive hydrogel using poly(vinyl alcohol)/polyethylene glycol/graphene oxide for human electrocardiogram acquisition, Polymers 9 (2017) 259.
[5] N. Luo, W. Dai, C. Li, Z. Zhou, L. Lu, C.C.Y. Poon, et al., Flexible piezoresistive sensor patch enabling ultralow power cuffless blood pressure measurement, Adv. Funct. Mater. 26 (2016) 1178–1187.
[6] K. Qi, J. He, H. Wang, Y. Zhou, X. You, N. Nan, et al., A highly stretchable nanofiber-based electronic skin with pressure-, strain-, and flexion-sensitive properties for health and motion monitoring, ACS Appl. Mater. Interfaces 9 (2017) 42951–42960.
[7] J. Huang, D. Li, M. Zhao, A. Mensah, P. Lv, X. Tian, et al., Highly sensitive and stretchable CNT-bridged agNP strain sensor based on TPU electrospun membrane for human motion detection, Adv. Electron. Mater. 5 (2019), 1900241.
[8] Y. Zang, F. Zhang, C.-A. Di, D. Zhu, Advances of flexible pressure sensors toward artificial intelligence and health care applications, Mater. Horiz. 2 (2015) 140–156.
[9] M. Dai, X. Xiao, X. Chen, H. Lin, W. Wu, S. Chen, A low-power and miniaturized electrocardiograph data collection system with smart textile electrodes for monitoring of cardiac function, Australas Phys. Eng. Sci. 39 (2016) 1029–1040.
[10] S.Y. Kim, S. Park, H.W. Park, D.H. Park, Y. Jeong, D.H. Kim, Highly sensitive and multimodal all-carbon skin sensors capable of simultaneously detecting tactile and biological stimuli, Adv. Mater. 27 (2015) 4178–4185.
[11] J. Wu, H. Wang, Z. Su, M. Zhang, X. Hu, Y. Wang, et al., Highly flexible and sensitive wearable e-skin based on graphite nanoplatelet and polyurethane nanocomposite films in mass industry production available, ACS Appl. Mater. Interfaces 9 (2017) 38745–38754.
[12] S. Li, Y. Gu, G. Wu, K. Dong, M. Jia, D. Zhang, X. Xiao, A flexible piezoresistive sensor with highly elastic weave pattern for motion detection, Smart Mater. Struct. 28 (2019), 035020.
[13] Y. Gao, M. Xu, G. Yu, J. Tan, F. Xuan, Extrusion printing of carbon nanotube-coated elastomer fiber withmicrostructures for flexible pressure sensors, Sens. Actuator. A-Phys. 299 (2019), 111625.
[14] G. Wu, S. Li, J. Hu, M. Dong, K. Dong, X. Hou, X. Xiao, A capacitive sensor using resin thermoplastic elastomer and carbon fibers for monitoring pressure distribution, Pigm. Resin Technol. 04 (2020), http://dx.doi.org/10.1108/PRT-10-2019-0098.
[15] X. Yang, Y. Wang, X. Qing, A flexible capacitive sensor based on the electrospun PVDF nanofibermembrane with carbon nanotubes, Sens. Actuator. A-Phys. 299 (2019), 111579.
[16] S. Li, T. Chen, X. Xiao, Periodically inlaid carbon fiber bundles in the surface of honeycomb woven fabric for fabrication of normal pressure sensor, J. Mater. Res. 55 (2020) 6551–6565.
[17] S. Miller, Z. Bao, Fabrication of flexible pressure sensors with microstructured polydimethylsiloxane dielectrics using the breath figures method, J. Mater. Res. 30 (2015) 3584–3594.
[18] S. Chen, Z. Lou, D. Chen, Z. Chen, K. Jiang, G. Shen, Highly flexible strain sensor based on ZnO nanowires and P(VDF-TrFE) fibers for wearable electronic device, Sci. China-Mater. 59 (2016) 173–181.
[19] Q. Li, T. Duan, J. Shao, H. Yu, Fabrication method for structured porous polydimethylsiloxane (PDMS), J. Mater. Sci. 53 (2018) 11873–11882.
[20] J. Lee, H. Kwon, J. Seo, S. Shin, J.H. Koo, C. Pang, et al., Conductive fiber-based ultrasensitive textile pressure sensor for wearable electronics, Adv. Mater. 27 (2015) 2433–2439.
[21] X. Sun, J. Sun, T. Li, S. Zheng, C. Wang, W. Tan, et al., Flexible tactile electronic skin sensor with 3D force detection based on porous CNTs/PDMS nanocomposites, Nano-Micro Lett. 11 (2019) 57.
[22] W. Obitayo, T. Liu, Effect of orientation on the piezoresistivity of mechanically drawn single walled carbon nanotube (SWCNT) thin films, Carbon 85 (2015) 372–382.

[23] J. Lee, S. Kim, J. Lee, D. Yang, B.C. Park, S. Ryu, et al., A stretchable strain sensor based on a metal nanoparticle thin film for human motion detection, Nanoscale 6 (2014) 11932–11939.
[24] J. Zhou, X. Xu, Y. Xin, G. Lubineau, Coaxial thermoplastic elastomer-wrapped carbon nanotube fibers for deformable and wearable strain sensors, Adv. Funct. Mater. 28 (2018), 1705591.
[25] K.F. Lei, K.-F. Lee, M.-Y. Lee, A flexible PDMS capacitive tactile sensor with adjustable measurement range for plantar pressure measurement Microsystem Technologies-Micro-And Nanosystems-Information Storage And Processing Systems, Vol. 20, 2014, pp. 1351–1358.
[26] K.F. Lei, K.-F. Lee, M.-Y. Lee, Development of a flexible PDMS capacitive pressure sensor for plantar pressure measurement, Microelectron. Eng. 99 (2012) 1–5.
[27] B.C.K. Tee, A. Chortos, R.R. Dunn, G. Schwartz, E. Eason, Z. Bao, Tunable flexible pressure sensors using microstructured elastomer geometries for intuitive electronics, Adv. Funct. Mater. 24 (2014) 5427–5434.
[28] T. Li, H. Luo, L. Qin, X. Wang, Z. Xiong, H. Ding, et al., Flexible capacitive tactile sensor based on micropatterned dielectric layer, Small 12 (2016) 5042–5048.
[29] S. Duan, K. Yang, Z. Wang, M. Chen, L. Zhang, H. Zhang, et al., Fabrication of highly stretchable conductors based on 3d printed porous poly(dimethylsiloxane) and conductive carbon nanotubes/graphene network, ACS Appl. Mater. Interfaces 8 (2016) 2187–2192.
[30] S. Wu, J. Zhang, R.B. Ladani, A.R. Rayindran, A.P. Mouritz, A.J. Kinloch, et al., Novel electrically conductive porous PDMS/carbon nanofiber composites for deformable strain sensors and conductors, ACS Appl. Mater. Interfaces 9 (2017) 14207–14215.
[31] Y. Kim, S. Jang, J.H. Oh, Fabrication of highly sensitive capacitive pressure sensors with porous PDMS dielectric layer via microwave treatment, Microelectron. Eng. 215 (2019), 111002.
[32] S. Kang, J. Lee, S. Lee, S. Kim, J.-K. Kim, H. Algadi, et al., Highly sensitive pressure sensor based on bioinspired porous structure for real-time tactile sensing, Adv. Electron. Mater. 2 (2016), 1600356.
[33] J.S. De, J.W. Snaith, N.A. Michie, A mechanical model for the lateral compression of woven fabrics, Text. Res. J. 56 (1986) 759–767.
[34] J. Pignanelli, K. Schlingman, T.B. Carmichael, S. Rondeau-Gagne, M.J. Ahamed, A comparative analysis of capacitive-based flexible PDMS pressure sensors, Sens. Actuator. A-Phys. 285 (2019) 427–436.

## Biographies

**Mr. Siming Li** received his B.Sc. degree in 2018 from the School of Textiles and Clothing, Jiangnan University, Wuxi (China). Currently, he is studying as a Master candidate at Jiangnan University. His research focuses on the development of wearable pressure sensors for e-textiles.

**Mr. Dong Ke** received his B.Sc. degree in 2018 from the School of Textiles and Clothing, Jiangnan University, Wuxi (China). Currently, he is studying at Jiangnan University as a Master candidate. His research focuses on 3D printing and shape memory polymer materials.

**Miss Ruiqing Li** received her B.Sc. degree in 2019 from the School of Textiles and Clothing, Jiangnan University, Wuxi (China). Currently, she is studying at Jiangnan University as a Master candidate. Her main research interests include advanced sensing technology.

**Miss Xiayan Huang,** undergraduate student of the School of Textiles and Clothing, Jiangnan University, Wuxi (China). Her main research interests include 3D printed structure materials inspired from weave structures.

**Miss Tianjiao Chen,** undergraduate student of the School of Textiles and Clothing, Jiangnan University, Wuxi (China). Her main research interests include sensors based on woven fabrics.

**Dr. Xueliang Xiao**, Associate Professor from the School of Textiles and Clothing, Jiangnan University, Wuxi (China). His research activity concerns with flexible sensor materials, smart wearable electronic clothing materials, shape memory polymers and fabric structural mechanics.